ZnO nanowires based piezoelectric transducers: the role of size and semiconducting properties

Thomas Jalabert, Manojit Pusty, Andrés Jenaro Lopez Garcia, Alessandro Cresti, Mireille Mouis, Gustavo Ardila

▶ **To cite this version:**

Thomas Jalabert, Manojit Pusty, Andrés Jenaro Lopez Garcia, Alessandro Cresti, Mireille Mouis, et al.. ZnO nanowires based piezoelectric transducers: the role of size and semiconducting properties. SPIE Optics + Optoelectronics, Apr 2023, Prague, Czech Republic. pp.1258406-1, 10.1117/12.2665500 . hal-04160671

HAL Id: hal-04160671
https://hal.science/hal-04160671

Submitted on 13 Jul 2023

HAL is a multi-disciplinary open access archive for the deposit and dissemination of scientific research documents, whether they are published or not. The documents may come from teaching and research institutions in France or abroad, or from public or private research centers.

L'archive ouverte pluridisciplinaire **HAL**, est destinée au dépôt et à la diffusion de documents scientifiques de niveau recherche, publiés ou non, émanant des établissements d'enseignement et de recherche français ou étrangers, des laboratoires publics ou privés.

ZnO nanowires based piezoelectric transducers: the role of size and semiconducting properties

T. Jalabert*[a], M. Pusty[a], A. J. Lopez Garcia[a,] A. Cresti[a], M. Mouis[a], G Ardila*[a]
[a]Univ. Grenoble Alpes, CNRS, Grenoble INP, IMEP-LaHC, F-38000 Grenoble, France
* Author contact : thomas.jalabert@grenoble-inp.fr, ardilarg@minatec.grenoble-inp.fr

Piezoelectric thin films are widely used in MEMS and NEMS actuators and resonators, but also in mechanical sensors and energy harvesters for IoT applications and Wireless Sensors Networks. Nanotechnology involving piezoelectric materials is a key research direction, with benefits expected from nanostructuring and the replacement of toxic materials. Piezoelectric nanocomposites based on semiconducting nanowires (NWs) are an alternative to thin films with nanostructuration benefits, such as low temperature fabrication and higher flexibility than thin films. In addition, they exhibit larger piezoelectric coefficient than their thin films counterparts. In this work we study the piezoelectric performance of vertically grown ZnO NWs based on Finite Element simulations in the PFM (Piezoresponse Force Microscopy) configuration. In this AFM (Atomic Force Microscope) mode, the AFM tip is placed in contact with the top surface of the NW while applying a voltage, thus inducing a deformation of the structure by the reverse piezoelectric effect. Different parameters are assessed: the effect of the surrounding air, the NW size and geometry and the effect of the semiconducting properties, in particular the doping level and surface traps density. The results are compared to previous theoretical approaches and experimental findings.

Keywords: Piezoresponse Force Microscopy, Finite Element Method, ZnO, nanowire, energy harvesting, piezoelectric coefficient

1. INTRODUCTION

Piezoelectricity is more prominent in nanowires (NWs) of some semiconductors as compared to their bulk counterparts [1], for this reason NWs are appealing for mechanical energy harvesting applications.[2–4] There are many piezoelectric semiconductors like GaN, AlN, CdS however ZnO presents different advantages as biocompatibility, abundance and it is easy to process, in particular many methods can be used to grow vertically aligned ZnO NWs (See Figure 1).[5–12] The semiconducting nature of these materials is expected to affect their piezoelectric performance. Doped NWs show strong piezoelectric damping due to the screening of electric polarization by free charge carriers.[13] The screening effect can be reduced by the surface Fermi-level pinning effect which originates from the presence of large densities of surface traps.[14] The relationship between the geometry and the semiconducting properties in semiconducting NWs is thus important for the performance optimization of piezoelectric devices made of them. Very recently, experimental findings on the impact of diameter on the electromechanical properties of piezoelectric semiconducting NWs have been reported on vertically aligned GaN [15] and ZnO [16] NWs using AFM techniques. In particular Piezoresponse Force microscopy (PFM) is an effective tool to study the converse piezoelectric effect (i.e., induced deformation by the application of an electric field) on individual NWs.[17–20] Other than the diameter effect, this technique also have evidenced recently a non-homogenous distribution of the piezoelectric response at the top surface of vertically aligned NWs.[21]

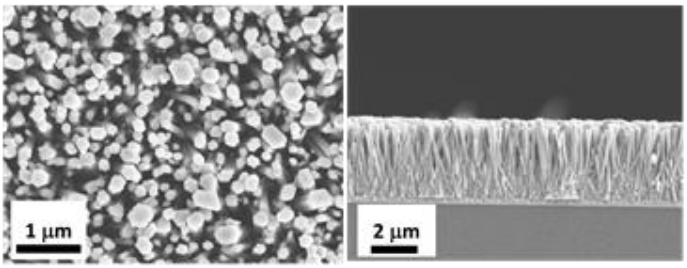

Figure 1. (a) SEM image of the top (left panel) and cross section (right panel) of typical ZnO NWs grown by CBD (Chemical Bath Deposition) [16].

From a theoretical point of view, the role of the length and diameter of the NWs on the direct piezoelectric effect (i.e., induced voltage by the application of strain) were studied for vertically integrated nanogenerators (VINGs), in particular including the surface trap density and doping levels.[22–24] The converse piezoelectric effect is rarely studied including the PFM configuration, where the free charge carriers and surface traps are excluded. However, it is found that the surface traps greatly affect the piezoelectric properties. The non-homogenous distribution of the piezoelectric response at the top surface of the NWs have been evaluated by simulations on 2D structures as an approximation and considering only doping concentrations.[21] More recently, the diameter effect has been explained by simulations on 3D axisymmetric structures (NWs) in PFM configuration. In these simulations, the AFM tip was considered in contact in the middle of the top surface of the NW. The simulations considered both the effect of surface traps densities and doping levels.[16]

The aim of this work is to deepen the theoretical study of the performance of vertically aligned ZnO NWs in the PFM configuration. Different environmental and geometrical parameters were studied: surrounding air, NW geometry, size and the semiconducting properties. Their effect in the global performance of the NWs is assessed and compared to previous theoretical and experimental results.

2. SIMULATION DETAILS

Static Finite element numerical simulations were performed under the COMSOL Multiphysics environment. Free charge carriers and surface traps were accounted for with user defined modifications to the set of equations given by the *Electrostatics* and *Solid Mechanics* modules. The simulated 3D structure is shown in Figure 2. It consists of a ZnO seed layer substrate, a ZnO NW and a metallic tip in air environment. The AFM tip was modeled by a 20nm thick cylinder with a 20nm radius, or by a cone with 20nm radius (R_{tip}) at its apex, a half angle of 10° (θ_{tip}) and a tip height (H_{tip}) of 1μm (see Figure 2). The seed layer was clamped to the bottom, and it was assumed that the tip was not affecting the mechanical movement of the NW. The electric permittivity of the tip was set to 1000 to highlight its metallic behavior. To maintain semiconductor neutrality in the seed layer the electric potential was set to zero at the bottom electrode and a voltage bias (V_0) was applied on the tip. The piezoelectric and semiconducting behavior of the NWs was explained by the following coupling equations:

$$[s] = [\mathbf{c}][\varepsilon] - [\mathbf{e}]^{\mathbf{T}}[\mathbf{E}] \quad (1)$$

$$[\mathbf{D}] = [\mathbf{e}][\varepsilon] + [\boldsymbol{\kappa}][\mathbf{E}], \quad (2)$$

where $[\sigma]$ is the stress matrix, $[\varepsilon]$ is the strain matrix, $[E]$ is the electric field vector, $[D]$ is the electric displacement vector, $[c]$ is the elasticity matrix, $[\kappa]$ is the dielectric constant matrix and $[e]$ is the piezoelectric coefficient. The terms $[e]$ and $[e]^T$ are matrices that introduces the coupling between the piezoelectric and semiconducting physics, that relates to the direct and the converse piezoelectric effect.

The local charge density (ρ) in Poisson's equation that includes the local free carrier densities and average doping concentrations is denoted by:

$$\nabla . D = \rho = e(p - n + N_d - N_a) \quad (3)$$

where, n, p, N_a and N_d are the densities of electrons, holes, acceptor atoms, and donor atoms respectively. The local electric potential and the band structures of the ZnO material, influenced the concentrations of electrons and holes.
The uniform trap density N_t was introduced at the ZnO surface, generating a surface charge density:

$$Q_s = -e^2 N_t (V_s - \varphi_{if}) \quad (4)$$

where V_s is the surface potential and φ_{if} is the difference between the Fermi level and the intrinsic level.[22] We assumed that the ideal traps would be slow and have a charge that remained frozen regardless of the applied voltage. Hence, the local surface voltage obtained in the initial state served as the basis for the boundary condition at ZnO contacts, resulting in a surface charge that was position-dependent but time-independent. Due to the application of an electric potential to

the tip from V_0^i = 0 to V_0^f = -1 V the top surface of the ZnO NW is displaced, from which the piezo response is calculated. The effective piezoelectric d_{33}^{eff} is found out by the division of the piezo response by $|V_0^f - V_0^i|$.

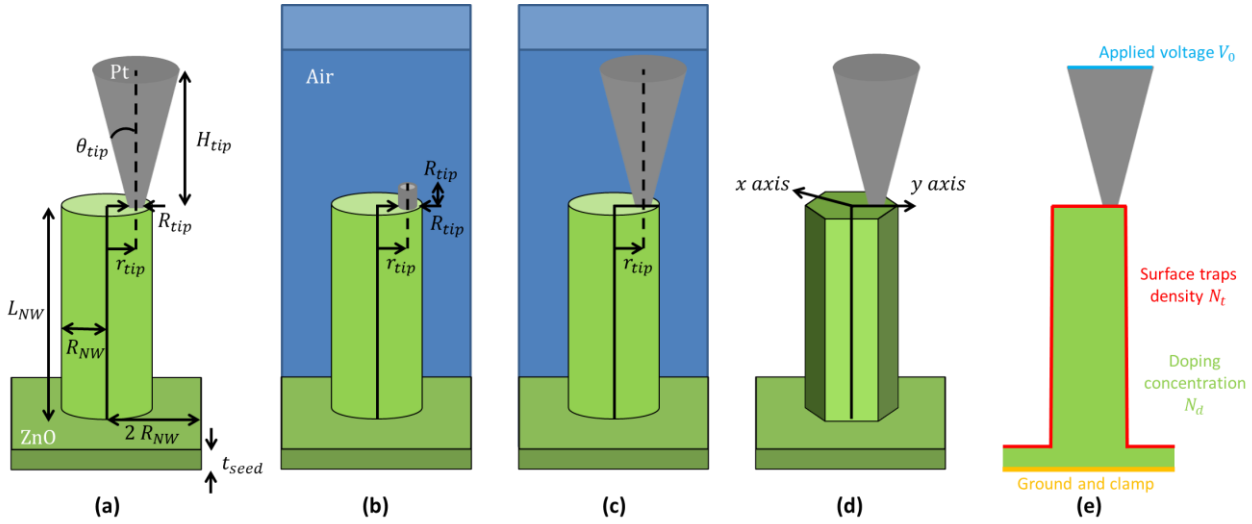

Figure 2. Schematics of the 3D numerical simulation of the deformation of a single NW by PFM within COMSOL environment in different configurations. (a) With a conical tip and without surrounding air, (b) with a cylindrical tip and with air and (c) with a conical tip ,air configuration and a cylindrical NW. (d) With a conical tip, without air and with a hexagonal NW configuration. (e) Cut view of the electrical and mechanical boundary conditions.

3. RESULTS AND DISCUSSION

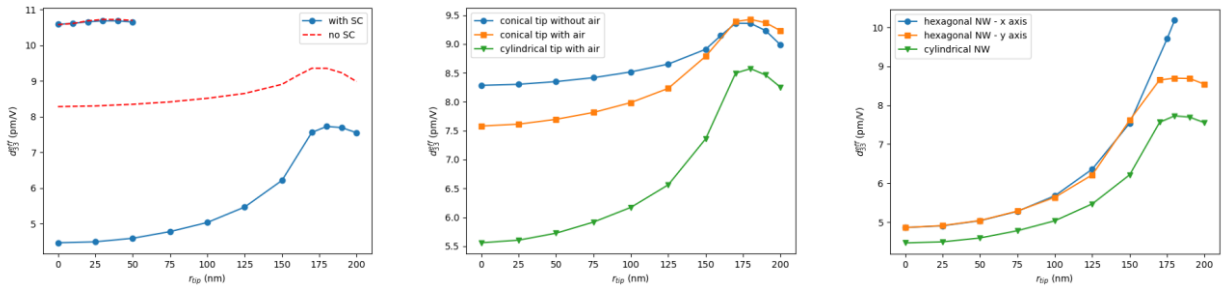

Figure 3. Simulated effective piezoelectric coefficient as a function of the position of the AFM tip across the NW surface for different simulation conditions. (a) 100 nm (top left) and 400 nm (bottom) diameter NW with (dots) and without (dashed lines) semiconducting properties in the Figure 2(a) configuration. (b) 400nm diameter NW without semiconducting properties in the configurations of Figure 2(a) (dots), 2(b) (triangles) and 2(c) (squares). (c) 400 nm diameter NW with semiconducting properties in the Figure 2(a) (triangles) and 2(d) (dots and squares) configurations. When semiconducting properties are included, $N_{it}=10^{13}$ $eV^{-1}.cm^{-2}$ *and* $N_d=10^{17}$ cm^{-3}.

Figure 3 shows the results of the computed effective piezoelectric coefficient with the different configurations of Figure 2. Figure 3(a) shows the piezoelectric coefficient as a function of tip position in the configuration of Figure 2(a) for two NW radii and with and without semiconducting properties. For a NW with small enough radius to reach full depletion, the computed piezoresponse is roughly independent on the tip position. In this case the response is also higher compared to the response of larger NWs. This is coherent with recent reports.[16,21] In this case, the semiconducting character of the NW does not change the computed piezoresponse. In contrast, for a NW with large enough radius so its core remains neutral despite surface depletion, the computed piezoresponse increases when the tip reaches the edge of

the NW. The magnitude of this increase is larger (about 35%) when considering the semiconducting character of the NW in comparison with the case without semiconducting properties (increase of about 10%).

Figure 3(b) shows the results for an insulating NW (without considering semiconducting properties) for the configurations of Figure 2(a), 2(b) and 2(c). The shape of the tip and the presence of air slightly affects the piezoresponse behavior but does not change the observed trend. Considering a conical AFM tip (which is closer to reality) reduces slightly the increase of the effective piezoelectric coefficient (about 15%) as the tip reaches the edge of the NW, in comparison to considering a simplified case of a cylindrical AFM tip (about 35%).

Figure 3(c) shows the results for the configurations of Figure 2(a) and 2(d) taking into consideration the semiconducting properties. The geometry of the NW (cylindrical or hexagonal) only slightly affects the piezoresponse.

Figure 4 compares the measured effective piezoelectric coefficient (or the equivalent piezoresponse) as a function of tip position with the theoretical prediction. Several piezoresponses versus tip position profiles along different directions are extracted from the experimental data.[16] They show an increase of the piezoresponse as the tip approaches the edge of the NW. This behavior is comparable with the predicted trend. The magnitude of the increase (about 30%) fits well the numerical simulations. The offset between experimental and theoretical values is probably due to a different level of doping density and surface traps density.

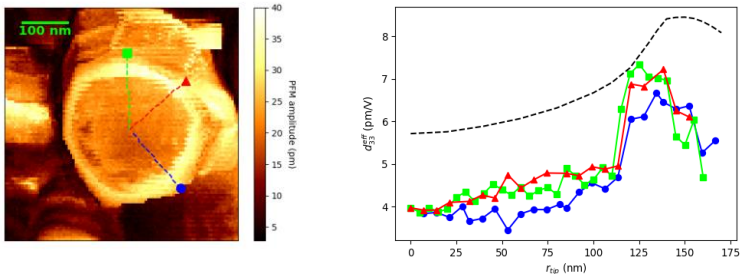

(a) (b)

Figure 4. Piezoresponse as a function of the position of the AFM tip across the NW surface. (a) 2D map of the piezoresponse. (b) Extracted effective piezoelectric coefficient along the lines drawn on (a) (dots) with simulated behavior corresponding to configuration of Figure 2 (a) (dashed line). The semiconducting parameters used in the simulation are the same as in Figure 3.

4. CONCLUSIONS

PFM is a powerful tool to characterize the piezoelectric performance of piezoelectric semiconducting NWs. Recent experiments using this AFM technique have shown important findings: an increasing performance (d_{33}^{eff} or effective piezoelectric coefficient) as the diameter of the NW decreases and a border effect in which the d_{33}^{eff} is not homogeneous at the top surface of the NW and increases as the AFM tip approaches its border. In this work we have improved the numerical simulations using finite element method in the PFM configuration to make them closer to the real conditions of the experiment. In particular by considering 3D structures in comparison to previous 2D or 3D axisymmetric approximations and by evaluating the effect of changing different parameters: (i) the diameter of the NW, (ii) the geometry of the NW (iii) the geometry of the AFM tip, (iv) the surrounding environment (air), (v) the position of the AFM tip at the surface of the NW and (vi) the influence of the semiconducting parameters (namely the doping level and the density of surface traps). Finally, the simulation trends have been compared to experimental data. The simulation trends correspond well to the experimental data although an offset of the data is present. This offset could be originated in particular because of a possible different level of doping or density of surface traps. This work demonstrates the need for additional experimental studies on trap density and carrier concentration in order to quantify more precisely their significance in transducers based on piezoelectric semiconducting NWs.

5. ACKNOWLEDGMENTS

This work has been partly supported by the ANR projects SCENIC (under grant agreement ANR-20-CE09-0005) and LATINO (under grant agreement ANR-21-CE50- 0026) from the French Ministry of Research. It also has been partly supported by the European Union's Horizon 2020 research and innovation programme projects PULSE-COM (under grant agreement No 863227) and ENABLES (under grant agreement no 730957).

6. REFERENCES

[1] Minary-Jolandan, M., Bernal, R. A., Kuljanishvili, I., Parpoil, V. and Espinosa, H. D., "Individual GaN nanowires exhibit strong piezoelectricity in 3D," Nano Lett. **12**(2), 970–976 (2012).

[2] Hu, Y., Lin, L., Zhang, Y. and Wang, Z. L., "Replacing a battery by a nanogenerator with 20 v output," Adv. Mater. **24**(1), 110–114 (2012).

[3] Wang, Z., Pan, X., He, Y., Hu, Y., Gu, H. and Wang, Y., "Piezoelectric Nanowires in Energy Harvesting Applications," Adv. Mater. Sci. Eng. **2015**, e165631 (2015).

[4] Panth, M., Cook, B., Zhang, Y., Ewing, D., Tramble, A., Wilson, A. and Wu, J., "High-performance strain sensors based on vertically aligned piezoelectric zinc oxide nanowire array/graphene nanohybrids," ACS Appl. Nano Mater. **3**(7), 6711–6718 (2020).

[5] Schmidt-Mende, L. and MacManus-Driscoll, J. L., "ZnO–nanostructures, defects, and devices," Mater. today **10**(5), 40–48 (2007).

[6] Nobis, T., Kaidashev, E. M., Rahm, A., Lorenz, M., Lenzner, J. and Grundmann, M., "Spatially inhomogeneous impurity distribution in ZnO micropillars," Nano Lett. **4**(5), 797–800 (2004).

[7] Yao, B. D., Chan, Y. F. and Wang, N., "Formation of ZnO nanostructures by a simple way of thermal evaporation," Appl. Phys. Lett. **81**(4), 757–759 (2002).

[8] Wu, J. and Liu, S., "Low-temperature growth of well-aligned ZnO nanorods by chemical vapor deposition," Adv. Mater. **14**(3), 215–218 (2002).

[9] Park, W. Il, Kim, D. H., Jung, S.-W. and Yi, G.-C., "Metalorganic vapor-phase epitaxial growth of vertically well-aligned ZnO nanorods," Appl. Phys. Lett. **80**(22), 4232–4234 (2002).

[10] Peulon, S. and Lincot, D., "Cathodic electrodeposition from aqueous solution of dense or open-structured zinc oxide films," Adv. Mater. **8**(2), 166–170 (1996).

[11] Vayssieres, L., Keis, K., Lindquist, S.-E. and Hagfeldt, A., "Purpose-built anisotropic metal oxide material: 3D highly oriented microrod array of ZnO," J. Phys. Chem. B **105**(17), 3350–3352 (2001).

[12] Consonni, V. and Lord, A. M., "Polarity in ZnO nanowires: A critical issue for piezotronic and piezoelectric devices," Nano Energy **83**, 105789 (2021).

[13] Romano, G., Mantini, G., Di Carlo, A., D'Amico, A., Falconi, C. and Wang, Z. L., "Piezoelectric potential in vertically aligned nanowires for high output nanogenerators," Nanotechnology **22**(46), 465401 (2011).

[14] Tao, R., Mouis, M. and Ardila, G., "Unveiling the influence of surface fermi level pinning on the piezoelectric response of semiconducting nanowires," Adv. Electron. Mater. **4**(1), 1700299 (2018).

[15] Gogneau, N., Chrétien, P., Sodhi, T., Couraud, L., Leroy, L., Travers, L., Harmand, J.-C., Julien, F. H., Tchernycheva, M. and Houzé, F., "Electromechanical conversion efficiency of GaN NWs: critical influence of the NW stiffness, the Schottky nano-contact and the surface charge effects," Nanoscale **14**(13), 4965–4976 (2022).

[16] Jalabert, T., Pusty, M., Mouis, M. and Ardila, G., "Investigation of the diameter-dependent piezoelectric response of semiconducting ZnO nanowires by Piezoresponse Force Microscopy and FEM simulations," Nanotechnology **34**(11), 115402–115409 (2023).

[17] Lozano, H., Catalan, G., Esteve, J., Domingo, N. and Murillo, G., "Non-linear nanoscale piezoresponse of single ZnO nanowires affected by piezotronic effect," Nanotechnology **32**(2), 25202 (2020).

[18] Jaloustre, L., Le Denmat, S., Auzelle, T., Azadmand, M., Geelhaar, L., Dahlem, F. and Songmuang, R., "Toward quantitative measurements of piezoelectricity in III-N semiconductor nanowires," ACS Appl. Nano Mater. **4**(1), 43–52 (2020).

[19] Garcia, A. J. L., Jalabert, T., Pusty, M., Defoor, V., Mescot, X., Montanino, M., Sico, G., Loffredo, F., Villani, F., Nenna, G. and Ardila, G., "Size and Semiconducting Effects on the Piezoelectric Performances of ZnO Nanowires Grown onto Gravure-Printed Seed Layers on Flexible Substrates," Nanoenergy Adv. **2**(2), 197–209

(2022).
[20] Scrymgeour, D. A. and Hsu, J. W. P., “Correlated piezoelectric and electrical properties in individual ZnO nanorods,” Nano Lett. **8**(8), 2204–2209 (2008).
[21] Garcia, A. J. L., Jalabert, T., Pusty, M., Defoor, V., Mescot, X., Montanino, M., Sico, G., Loffredo, F., Villani, F. and Nenna, G., “Size and semiconducting effects on the piezoelectric performances of ZnO nanowires grown onto gravure-printed seed layers on flexible substrates,” Nanoenergy Adv. **2**(2), 197–209 (2022).
[22] Garcia, A. J. L., Mouis, M., Consonni, V. and Ardila, G., “Dimensional roadmap for maximizing the piezoelectrical response of ZnO nanowire-based transducers: impact of growth method,” Nanomaterials **11**(4), 941–959 (2021).
[23] Garcia, A. J. L., Mouis, M., Cresti, A., Tao, R. and Ardila, G., “Influence of slow or fast surface traps on the amplitude and symmetry of the piezoelectric response of semiconducting-nanowire-based transducers,” J. Phys. D. Appl. Phys. **55**(40), 405502 (2022).
[24] Lopez Garcia, A. J., Mouis, M., Jalabert, T., Cresti, A. and Ardila, G., “Length and polarity dependent saturation of the electromechanical response of piezoelectric semiconducting nanowires,” J. Phys. D. Appl. Phys. **56**(12), 125301 (2023).